



Hydrodynamics of monolayer domains at the air–water interface

David K. Lubensky and Raymond E. Goldstein

Citation: *Physics of Fluids* **8**, 843 (1996); doi: 10.1063/1.868893

View online: <http://dx.doi.org/10.1063/1.868893>

View Table of Contents: <http://scitation.aip.org/content/aip/journal/pof2/8/4?ver=pdfcov>

Published by the [AIP Publishing](#)

Articles you may be interested in

[Organization in pure and alternate deuterated cadmium arachidate monolayers on solid substrates and at the air/water interface studied by conventional and differential Fourier transform infrared spectroscopies](#)

J. Chem. Phys. **104**, 9983 (1996); 10.1063/1.471726

[The stability of bicontinuous microemulsions: A molecular theory of the bending elastic properties of monolayers comprised of ionic surfactants and nonionic cosurfactants](#)

J. Chem. Phys. **103**, 4765 (1995); 10.1063/1.470612

[Dual beam spectrometer for optical studies of spread monolayers at the air–water interface](#)

Rev. Sci. Instrum. **65**, 2781 (1994); 10.1063/1.1144616

[A nonleak trough for monolayers at the air/water interface](#)

Rev. Sci. Instrum. **65**, 500 (1994); 10.1063/1.1145164

[Surface density of soluble surfactants at the air/water interface: Adsorption equilibrium studied by second harmonic generation](#)

J. Chem. Phys. **95**, 4620 (1991); 10.1063/1.461730

PHYSICS
TODAY

Welcome to a

Smarter Search



with the redesigned
Physics Today Buyer's Guide

Find the tools you're looking for today!

Hydrodynamics of monolayer domains at the air–water interface

David K. Lubensky^{a),b)}

*Department of Physics, Joseph Henry Laboratories, Princeton University, Princeton, New Jersey 08544
and Institut Charles Sadron, 6 rue Boussingault, 67083 Strasbourg Cedex, France*

Raymond E. Goldstein^{c)}

Department of Physics, Joseph Henry Laboratories, Princeton University, Princeton, New Jersey 08544

(Received 1 September 1995; accepted 20 December 1995)

Molecules at the air–water interface often form inhomogeneous layers in which domains of different densities are separated by sharp interfaces. Complex interfacial pattern formation may occur through the competition of short- and long-range forces acting within the monolayer. The overdamped hydrodynamics of such interfacial motion is treated here in a general manner that accounts for dissipation both within the monolayer and in the subfluid. Previous results on the linear stability of interfaces are recovered and extended, and a formulation applicable to the nonlinear regime is developed. A simplified dynamical law valid when dissipation in the monolayer itself is negligible is also proposed. Throughout the analysis, special attention is paid to the dependence of the dynamical behavior on a characteristic length scale set by the ratio of the viscosities in the monolayer and in the subphase. [S1070-6631(96)01804-8] © 1996 American Institute of Physics.

I. INTRODUCTION AND EXPERIMENTAL BACKGROUND

Molecular layers of surfactants or polymers at the air–water interface are often found in inhomogeneous states within which appear domains of nearly uniform density.^{1,2} In many ways, these states resemble conventional two-phase coexistence regions with sharp interfaces between different homogeneous phases; because of long-range electrostatic interactions within the monolayer, however, domains of a given phase can be stable rather than coarsening in time.³ Experimentally observed domains typically have sizes of 10–100 μm .

A considerable body of experimental^{4–12} and theoretical^{13–15} work has focused on the motion of the domain boundaries. These investigations have had two complementary motivations. On the one hand, the boundary dynamics provide a means of probing physical parameters, such as the line tension between phases, that are otherwise difficult to measure.^{7,12,15} On the other, the electrostatic interactions are caused by the molecules' permanent dipoles that are oriented with respect to the surface of the water; their mutual repulsion can result in intricate fingering instabilities that have parallels in a variety of other pattern-forming systems.³ The laws of motion of the interfaces between monolayer phases have been probed directly in experiments monitoring the relaxation of domains to a circular ground state, starting either from an elongated “bola” shape^{7,12} or from smaller elliptical deformations.^{9,12} The fastest-growing mode at the onset of a fingering instability has also been examined.^{4,5,11}

The complete interpretation of such experiments requires an understanding of the hydrodynamics of thin layers coupled to a subfluid. Some progress has been made in the analysis of particular cases. Building on earlier work on the diffusion of a cylinder embedded in a membrane,¹⁶ Stone and McConnell have solved the linearized boundary dynamics about a circle.^{13,14} Schwartz, Knobler, and Bruinsma¹⁷ and Stone¹⁸ have examined the flow of monolayers through channels. The related problem of fingering in quasi-two-dimensional domains of ferrofluids has also recently been considered,^{19–23} as has the behavior of capillary waves in the presence of coexisting monolayer phases.²⁴ The more general treatment of boundary motion applicable to a domain of any shape has, however, remained an open problem of considerable interest.

In this paper, we adapt boundary integral techniques from fluid mechanics²⁵ to the study of thin layers resting on a subfluid. Our approach is applicable to arbitrary geometries, and hence offers several advantages over techniques based on eigenfunction expansions that are useful only in particular situations with a high degree of symmetry. It allows the comparatively straightforward calculation of linearized growth rates about any number of stable shapes; it is also a starting point for the detailed investigation of the boundary dynamics in the nonlinear regime. Further, by separating those aspects of the problem that depend on energetics from those determined by the hydrodynamic equations, we gain several physical insights. Finally, our formulation provides a new example of a dynamical law governing curve motion in the plane. It is thus of interest to the broader study of pattern formation.

In Sec. II, we present a formulation of the boundary dynamics valid for arbitrary viscosities and subfluid depths, and note some global properties of the resulting dynamical

^{a)}Present address: Department of Physics, Harvard University, Cambridge, Massachusetts 02138.

^{b)}Electronic mail: lubensky@fas.harvard.edu

^{c)}Electronic mail: gold@davinci.princeton.edu

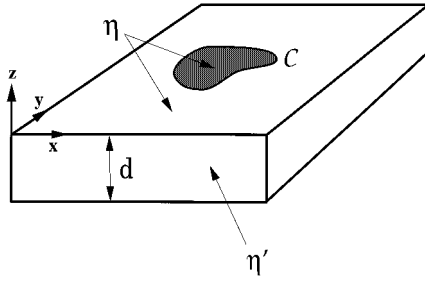


FIG. 1. Schematic of the system studied, in which an interface C exists within a monolayer of viscosity η resting on top of a subphase with viscosity η' and depth d .

law. In Sec. III we consider in greater detail the more analytically tractable limiting cases of an infinitely deep or very thin subfluid. In Sec. IV, we examine the linear stability of straight and circular boundaries. Drawing on these results, in Sec. V we propose a simplified dynamics appropriate when dissipation occurs mostly in the subfluid. This limiting form has the intriguing feature that it contains a local drag term at the interface not unlike that introduced in the Rouse model of polymer dynamics.²⁶ In Sec. VI we give a brief, illustrative calculation in the nonlinear regime, and in Sec. VII we discuss some limitations and possible extensions of our work.

II. GENERAL FORMULATION

A. The model and a boundary integral formulation

We begin by ignoring the presence of domains and studying a homogeneous two-dimensional layer coupled to a water subphase. The geometry of the system is shown in Fig. 1. Both fluids are taken to have an infinite horizontal extent, while the subphase may have a finite depth d . The monolayer is assumed to be an incompressible, Newtonian fluid with surface viscosity η (dimensions mass/time) filling the plane $z=0$.²⁷ It rests on a three-dimensional incompressible fluid of viscosity η' [dimensions mass/(length \times time)] that occupies the region $-d < z < 0$. All variables referring to the subfluid are primed. Since the Reynolds numbers involved in the slow relaxation of micron-scale domains seldom exceed 10^{-4} , we are justified in working in the overdamped limit. Neglecting all inertial terms in the Navier–Stokes equation, we then find that the system is governed by the two coupled Stokes equations,

$$\eta \nabla^2 \mathbf{u} - \nabla p + \mathbf{F}^S = \mathbf{0} \quad (1)$$

and

$$\eta' \nabla^2 \mathbf{u}' - \nabla p' = \mathbf{0}, \quad (2)$$

along with the incompressibility conditions $\nabla \cdot \mathbf{u} = 0$ and $\nabla \cdot \mathbf{u}' = 0$. The term \mathbf{F}^S gives the body force that the subfluid exerts on the monolayer. Note that the monolayer is treated as a truly two-dimensional fluid, so p is a surface pressure with dimensions of force/length. The two fluids are also linked by no-slip boundary conditions; these simply require that, at $z=0$, $\mathbf{u}_\perp = \mathbf{u}$ and $\mathbf{u}' \cdot \hat{\mathbf{z}} = 0$, where the \perp indicates the in-plane component of a three-dimensional vector. In addition,

we demand that all velocities vanish at infinity, and we impose no-slip boundary conditions on the bottom of the subfluid trough. Our model is thus essentially the same as that first introduced by Saffman to model flow in fluid membranes;²⁸ its predictions have been shown to agree well with experiment for monolayers flowing through a channel.¹⁷ The form of the force \mathbf{F}^S is determined by the subfluid's Newtonian stress tensor evaluated at $z=0$. The no-slip boundary conditions on the velocity field \mathbf{u}' imply that all terms containing $\mathbf{u}' \cdot \hat{\mathbf{z}}$ or its derivatives vanish, leaving the simple expression

$$\mathbf{F}^S = -\eta' \left. \frac{\partial \mathbf{u}'_\perp}{\partial z} \right|_{z=0}. \quad (3)$$

The presence of a domain boundary will modify the equations for flow in a homogenous layer. We describe the interface as a closed curve C in the $x-y$ plane (Fig. 1) and ask that the fluid velocity be continuous across this boundary. In order to make the problem more tractable, we also assume that the two monolayer phases separated by the interface possess the same viscosity; this assumption will be discussed further later in this section. With the curve is associated a parametrization $\mathbf{r}(\alpha)$ and an energy $\mathcal{E}[\mathbf{r}]$ that is a functional of $\mathbf{r}(\alpha)$. In the simplest case in which there exists only a line tension γ , for example, $\mathcal{E}[\mathbf{r}] = \gamma \int ds$, where $ds = \sqrt{g} d\alpha$, and $\sqrt{g} \equiv |d\mathbf{r}/d\alpha|$ is the metric factor.

To understand the effect of an interfacial force, we next introduce the Green's function G_{ij} that gives the response of a monolayer *coupled to a subfluid* to a point force exerted on the monolayer. A force \mathbf{g} acting at the origin will induce a velocity field \mathbf{u}^g in the monolayer that is related to the Green's function by

$$u_i^g(\mathbf{r}) = \frac{1}{4\pi\eta} G_{ij}(\mathbf{r}) g_j, \quad (4)$$

where summation over repeated indices is implied. One can similarly introduce Green's functions for the pressure and the body force exerted by the subfluid, defined by the relations

$$p^g(\mathbf{r}) = \frac{1}{4\pi} P_j(\mathbf{r}) g_j \quad \text{and} \quad F_i^S(\mathbf{r}) = \frac{1}{4\pi} f_{ij}^S(\mathbf{r}) g_j. \quad (5)$$

Together, the three will satisfy the equations

$$\nabla^2 G_{ij} - \partial_i P_j + f_{ij}^S = -4\pi \delta_{ij} \delta(\mathbf{r}), \quad (6a)$$

$$\partial_i G_{ij} = 0. \quad (6b)$$

The first of these equations is the analog for the Green's functions of equation (1) governing flow in the monolayer, while the second reproduces an incompressibility constraint. One could of course also write down the equations corresponding to the subfluid Stokes equation (2) and to the expression (3) for \mathbf{F}^S , but they are not necessary for the further development of the present paper.

For our purposes, the essential feature of an interface is that it exerts a force on the surrounding fluid. To find the velocity field in the presence of an interface, one must thus sum the contributions from the forces it exerts at each point. In other words,

$$u_j(\mathbf{r}) = -\frac{1}{4\pi\eta} \int_C ds G_{ij}(\mathbf{r}-\mathbf{r}(s)) \Delta f_i(\mathbf{r}(s)), \quad (7)$$

where we have chosen the sign convention that $\Delta \mathbf{f}$ is the net force per unit length that the fluid exerts on the interface. With equation (7), we have effectively reduced the problem of solving the two coupled partial differential equations (1) and (2) to that of finding the correct Green's function; although equation (7) makes no explicit reference to the subfluid, it is included implicitly because its presence determines the form of G_{ij} . Virtual work arguments give an expression for $\Delta \mathbf{f}$ in terms of $\delta[\mathbf{r}]$; when a small element of the surface is moved slightly, the stresses in the surrounding molecular layer must do work to change δ . The balance is expressed by the relation

$$\Delta \mathbf{f} = \frac{1}{\sqrt{g}} \frac{\delta \mathcal{E}}{\delta \mathbf{r}}, \quad (8)$$

which is simply a generalization of the well-known Young–Laplace formula for the force exerted by a tense interface. The preceding two equations are the basis for all of our subsequent treatment of boundary motion. With them, we can calculate \mathbf{u} anywhere in the plane; in particular, the values of \mathbf{u} on C give the interfacial velocity. Observe that the boundary velocity is always determined *nonlocally*, and so depends on the shape of the entire domain.

Equation (7) for the fluid velocity can also be derived by a more formal route²⁵: In the spirit of textbook solutions of Laplace's equation,²⁹ one begins by proving a reciprocal identity relating two arbitrary flows \mathbf{u} and \mathbf{v} . Choosing \mathbf{v} to be proportional to G_{ij} , one finds that the limiting value of \mathbf{u} as it approaches the boundary C of an arbitrary region is

$$u_j(\mathbf{r}) = -\frac{1}{2\pi\eta} \int_C ds G_{ij}(\mathbf{r}-\mathbf{r}(s)) f_i(\mathbf{r}(s)) - \frac{1}{2\pi} \int_C ds u_i(\mathbf{r}(s)) T_{ijk}(\mathbf{r}-\mathbf{r}(s)) n_k(\mathbf{r}(s)), \quad (9)$$

where f_i is the force that the fluid inside C exerts on C , n_k is a component of the unit normal vector, and $T_{ijk} \equiv -\delta_{ik} P_j + \partial_k G_{ij} + \partial_i G_{kj}$ is the Green's function for the stress tensor. In the case in which the viscosities inside and outside C are equal, one can readily combine the expressions for the limits from the inside and the outside to recover equation (7). When the two viscosities are different, this approach does not generally work: G_{ij} and T_{ijk} can depend on η , so terms containing the Green's functions for the inside and outside regions cannot necessarily be combined and cancelled. Hence, except in certain limits, our theory cannot immediately be extended to include viscosity contrast. Because of the difficulty of measuring the viscosities of individual phases in the region of coexistence, the importance of such contrast is usually not known. In most systems of interest, dissipation in the monolayer is negligible compared to dissipation in the bulk,^{12,30} suggesting that viscosity differences may not introduce too strong an effect. Likewise, in the opposite limit in which the subfluid is completely ignored, G_{ij} does not depend on η . The viscosity then enters

the problem only through the factors of $1/\eta$ in front of the integral in equation (9), and a little algebra makes it possible to deal with variations in η . It has been our experience that, in this case, the correction term due to viscosity contrast usually vanishes to linear order. Nonetheless, a more complete theory would allow for the possibility of viscosity differences between phases.

Before turning to the calculation of G_{ij} , we remark lastly that our curve evolution dynamics produces a gradient flow in configuration space. That is, the energy \mathcal{E} associated with an interface will always decrease monotonically in time, with $d\mathcal{E}/dt$ precisely given by the sum of the rates of viscous dissipation in the monolayer and in the subfluid. To prove this, we begin by observing that $\Delta \mathbf{f} = \Delta \boldsymbol{\sigma} \cdot \hat{\mathbf{n}}$, where $\Delta \boldsymbol{\sigma}$ is the difference in stress tensors across the interface. The time derivative of the energy is then $d\mathcal{E}/dt = \int ds (\delta \mathcal{E} / \delta \mathbf{r}) \cdot \mathbf{u} = \int ds \hat{\mathbf{n}} \cdot \Delta \boldsymbol{\sigma} \cdot \mathbf{u}$. The divergence theorem allows one to transform this integral into an integral over the plane; by using the dynamical equation (1), one can then make terms in \mathbf{F}^S appear that can by similar arguments be written in terms of integrals over the subfluid volume. Ultimately, one finds that

$$\frac{d\mathcal{E}}{dt} = -2\eta \int d^2 \mathbf{r} (e_{ij})^2 - 2\eta' \int d^3 \mathbf{r}' (e'_{ij})^2, \quad (10)$$

where $e_{ij} = (\partial_i u_j + \partial_j u_i)/2$ is proportional to the viscous part of the stress tensor in the monolayer, and a similar definition holds for e'_{ij} in the subfluid. Summation over repeated indices is implied. The two integrals give, respectively, the rates of viscous dissipation in the monolayer and in the subfluid. The result is hardly surprising, but it has potentially important consequences for the pattern forming properties of the model: The system is constrained always to move “down-hill” in the space of shapes, so it will tend to get caught in metastable minima, and many shapes will be inaccessible to it.

B. Calculation of the Green's function

To find G_{ij} , we begin by finding the velocity field in the subfluid induced by an arbitrary flow in the monolayer; we will then proceed to calculate \mathbf{F}^S for this velocity field and finally to solve for the Green's function. The first task is greatly simplified by an observation of Stone and McConnell,¹³ who showed that when the monolayer velocity field is incompressible the subfluid pressure p' is constant. Though their proof only holds for an infinite subfluid, it can readily be extended to the case where the depth is finite; the result can also be verified independently starting from the expression for the subfluid velocity as an integral over the plane $z=0$.²⁵ With a constant pressure, $\nabla p' = \mathbf{0}$, and each component of \mathbf{u}' becomes harmonic. Solving for \mathbf{u}' is thus reduced to an exercise in electrostatics. Because the system is invariant with respect to translations in the monolayer plane, the drag force must take the form

$$\mathbf{F}^S(\mathbf{r}_0) = \frac{\eta'}{4\pi} \int d^2 \mathbf{r} K(\mathbf{r}_0 - \mathbf{r}) \mathbf{u}(\mathbf{r}), \quad (11)$$

where K is the derivative with respect to z of the appropriate Green's function for Laplace's equation. Both K and \mathbf{u} are functions defined on the plane. When the depth $d \rightarrow \infty$, K is readily obtained by the method of images; the extension to the case of a finite depth is treated in Appendix A. It turns out to be convenient to proceed in Fourier space. Denoting the Fourier transform (in two dimensions) of a function by a hat and adopting the convention that $f(\mathbf{r}) = \int d^2\mathbf{q} \hat{f}(\mathbf{q}) \times \exp(i\mathbf{q} \cdot \mathbf{r})$, we find that

$$\hat{K}(\mathbf{q}) = -\frac{q}{\pi} \coth(qd), \quad (12)$$

whence by the convolution theorem

$$\hat{\mathbf{F}}^S(\mathbf{q}) = -\eta' q \coth(qd) \hat{\mathbf{u}}(\mathbf{q}). \quad (13)$$

The obvious next step is to take the Fourier transform of the Green's function equation (6a). Making use of the fact that $\nabla \cdot \mathbf{u} = 0$, one can obtain an expression for \hat{P}_j and thus show that

$$\hat{G}_{ij}(\mathbf{q}) = \frac{q^2 \delta_{ij} - q_i q_j}{\pi q^2 [q^2 + a q \coth(qd)]}. \quad (14)$$

The parameter a is the ratio of the viscosities of the subphase and the monolayer,

$$a \equiv \frac{\eta'}{\eta}, \quad (15)$$

and has dimensions of inverse length. This parameter plays a fundamental role in all subsequent analyses. When multiplied by an appropriate length scale, it will be the governing dimensionless parameter of the problem.

The form of the expression for \hat{G}_{ij} suggests that we define the differential operator,

$$D_{ij} \equiv -\frac{1}{\pi} (\delta_{ij} \nabla^2 - \partial_i \partial_j) \quad (16)$$

so that we can write G_{ij} in terms of a single scalar function as

$$G_{ij} = D_{ij} H(\mathbf{r}), \quad (17)$$

with

$$\hat{H}(\mathbf{q}) = \frac{1}{q^2 [q^2 + a q \coth(qd)]}. \quad (18)$$

In principle, we could now invert this transform and calculate G_{ij} . In practice, the result would be so cumbersome as to be useless. Instead, in the next section we will study the behavior of \hat{H} in several different limits.

III. LIMITING CASES

In this section, we will consider the behavior of the model in the limits of large and small a and d . Since both of these variables have dimensions, we must compare them with some other quantity to have a meaningful notion of "large" and "small." The only candidate that presents itself in the present formulation is the wavevector q . If the system under consideration has a single length scale L , then the most important contributions in Fourier space are likely to

come at $q \sim 1/L$, and the relevant dimensionless parameters are d/L and aL . This would be the case, for example, for a circular domain of radius R whose boundary was smooth on all smaller scales; we would then have $L \sim R$. We caution, however, that $q \sim 1/L$ is at best a rough estimate and that q must actually be allowed to range from zero to infinity. Hence, great care must be exercised in taking limits when there is more than one candidate for L . This is particularly true when an approximation is valid only for large enough L , for there is always the danger that the domain boundary will finger or develop roughness at smaller length scales. For example, the important length scale in the case of a circle subject to n -fold harmonic perturbations is not its radius R but the wavelength $2\pi R/n$; whether or not a given approximation is valid thus depends on the mode one is considering.

A. Infinite subfluid

We begin by considering the case of a very deep subfluid, $qd \rightarrow \infty$. This is usually the experimentally relevant limit, for typical troughs have depths on the order of millimeters, while the monolayer domains observed tend to be on the scale of tens, or at most hundreds of microns.³¹ In this limit, $\coth(qd) \rightarrow 1$, and \hat{H} takes the simplified form

$$\hat{H}(\mathbf{q}) = \frac{1}{q^3(q+a)}. \quad (19)$$

Note that in the limit of large q/a , \hat{H} behaves as q^{-4} , while in the limit of small q/a it behaves as q^{-3} ; these should determine the behavior of G_{ij} at small and large r , respectively. If one lets $q/a \rightarrow \infty$, or equivalently sets $a=0$, one recovers the case of a purely two-dimensional layer without any coupling to a bulk fluid. Although the integrals required to take the inverse transform of q^{-4} diverge in the usual sense, they can be dealt with by the theory of generalized functions.^{32,33} Essentially, all that is required is the introduction of a convergence factor like that commonly used to treat quantum-mechanical scattering from a Coulomb potential. One then finds that

$$H(\mathbf{r}) = \frac{\pi}{2} r^2 \ln(r) \quad (20)$$

and

$$G_{ij}(\mathbf{r}) = -\delta_{ij} \ln(r) + \frac{r_i r_j}{r^2}, \quad (21)$$

where r_i is a component of \mathbf{r} . This is precisely the two-dimensional "Stokeslet" of fluid mechanics.^{25,34} Although one should generally not take the logarithm of a quantity with dimensions, in the above equations this transgression turns out to be without consequences. With $a=0$, the system has no intrinsic length scale, and we can choose to divide r by whatever length we please; the only change will be in an unimportant additive constant corresponding to a Galilean transformation.

It is tempting to try to treat the limit in which dissipation in the subfluid dominates in the same manner just used for the case in which it is negligible. Unfortunately, if one blithely takes the inverse transform of $1/(aq^3)$, obtaining

$-2\pi r/a$, and proceeds to calculate a Green's function, clearly unphysical results emerge. In the simplest terms, one can argue that this occurs because the limit of large q/a will break down at large distances, a feature that is acceptable for finite size domains, while the limit of small q/a becomes invalid precisely at the small distances that one must always consider. More specifically, the limit $a \rightarrow \infty$ corresponds to neglecting the term $\eta \nabla^2 \mathbf{u}$ in the dynamical equation (1). One is then left with a lower order equation for which one is allowed to impose fewer boundary conditions, so the integral formulation of equation (7) can no longer hold. We will argue in Section V that these difficulties can be circumvented with the judicious use of cut-offs.

To proceed further within the present framework, however, one must deal with the form for \hat{H} valid for arbitrary a . A fairly involved expression for the inverse transform is obtained in Appendix B; it can be expanded about $ar=0$ to give

$$H(\mathbf{r}) = \frac{\pi}{a^2} \left[\frac{4C - 3 + 4 \ln(ar/2)}{8} (ar)^2 - \frac{2}{9} (ar)^3 + \frac{1 - C - \ln(ar/2)}{32} (ar)^4 + \dots \right], \quad (22)$$

where $C \approx 0.577$ is Euler's constant. Since $D_{ij}r^2 = 2\delta_{ij}$, the term proportional to r^2 will add a constant velocity to G_{ij} . Unlike in the case $a=0$, such a constant now has a physical meaning; the presence of the subfluid destroys Galilean invariance.

B. Thin subfluid

We next turn to the case of a very thin subfluid layer, $qd \rightarrow 0$ or $d/L \rightarrow 0$. Although no experiments have yet been conducted in this regime, it seems plausible that it might be experimentally accessible. In numerical studies of monolayer flow in canals, for example, Stone has observed that the effects of finite depth become important when $d \sim L$.¹⁸ For the largest experimentally accessible monolayer domains, a trough with a depth $d \sim 100 \mu\text{m}$ would then be required; this seems mechanically conceivable, although reflection from the bottom of the trough might make visualization with some microscopy techniques difficult.¹² Beyond the fact that its theoretical treatment is less involved, this limit has the potential advantage that it would give the experimenter, in the depth d , an additional parameter that could be controlled with a fair degree of precision. For example, Klinger and McConnell have reported the ability to set d to within $1 \mu\text{m}$.³¹

To lowest order in qd , \hat{H} takes the form

$$\hat{H} = \frac{1}{q^2(q^2 + \lambda^2)}, \quad \lambda^2 \equiv \frac{a}{d} = \frac{\eta'}{\eta d}. \quad (23)$$

The parameter λ plays the same role as a in the infinite subfluid problem. The inverse transform of \hat{H} can be taken without great difficulty and a Green's function obtained. It turns out to be more instructive, however, to back up several steps and to consider the function K introduced in the previ-

ous section. Expanding the Fourier transform of K , inverting, and taking the convolution with \mathbf{u} , we obtain

$$\hat{K}(\mathbf{q}) = -\frac{1}{\pi d} \left[1 + \frac{1}{3}(qd)^2 + \dots \right], \quad (24a)$$

$$K(\mathbf{r}) = -\frac{4\pi}{d} \left[\delta(\mathbf{r}) + \frac{1}{3}d^2 \nabla^2 \delta(\mathbf{r}) + \dots \right], \quad (24b)$$

$$\mathbf{F}^S = -\frac{\eta'}{d} \left[\mathbf{u} + \frac{1}{3}d^2 \nabla^2 \mathbf{u} + \dots \right]. \quad (24c)$$

The first term in the expansion of \mathbf{F}^S has been derived by Stone via more heuristic arguments^{14,18}; it is also the expression for \mathbf{F}^S that one obtains by treating the subfluid in the lubrication approximation. In qualitative terms, the series tells us that as d increases the force exerted by the subfluid develops an increasingly nonlocal character. For very small d , the no-slip boundary conditions on the bottom of the trough completely dominate the behavior and prevent the effects of motion in the monolayer from propagating through the subfluid. As d increases, however, different parts of the adsorbed layer become more and more able to communicate with each other through the subfluid. In the opposite limit of infinite depth, we thus expect that \mathbf{F}^S will depend on the velocity field throughout the monolayer.

We confine ourselves for the moment to considering only the leading term in the above expansions. It is of course also possible to look at higher order approximations, but they lack the internal consistency of the lowest order dynamics. In particular, they will not always yield a law of motion that is a gradient flow. In the first approximation, a comparatively simple equation holds:

$$\eta \nabla^2 \mathbf{u} - \nabla p - \frac{\eta'}{d} \mathbf{u} = \mathbf{0}. \quad (25)$$

This equation has the same form as the Laplace transform with respect to time of the linearized Navier–Stokes equation $\rho \partial \mathbf{u} / \partial t = \eta \nabla^2 \mathbf{u} - \nabla p$ and has been studied in this context²⁵; it has also been used to model flow in porous media.³⁵ If we ignore dissipation in the monolayer entirely compared with dissipation in the subfluid, the equation reduces to Darcy's law $\mathbf{u} \propto -\nabla p$, which describes quasi-two-dimensional flow in Hele–Shaw cells.^{22,23} The Green's function for Eq. (25) has previously been calculated²⁵ and can readily be obtained by taking the inverse transform of equation (23). One finds that

$$H(\mathbf{r}) = -\frac{2\pi}{\lambda^2} [\ln(\lambda r) + K_0(\lambda r)] \quad (26)$$

and

$$G_{ij}(\mathbf{r}) = -2\delta_{ij} \left[\frac{1}{(\lambda r)^2} - K_0(\lambda r) - \frac{K_1(\lambda r)}{\lambda r} \right] + 2 \frac{r_i r_j}{r^2} \left[\frac{2}{(\lambda r)^2} - K_0(\lambda r) - \frac{2K_1(\lambda r)}{\lambda r} \right], \quad (27)$$

where K_i is a modified Bessel function. Note that in the limit $\lambda r \rightarrow 0$, H approaches the expression obtained in the complete absence of a subfluid. Close enough to a singularity, the

presence of the subfluid will always be negligible because the higher order derivative $\nabla^2 \mathbf{u}$ will always dominate \mathbf{F}^S .

IV. LINEAR STABILITY

While the present formulation of the monolayer hydrodynamics permits the investigation of boundary motion far from any regular geometric shape, where a fully nonlinear analysis is necessary, we focus here on the calculation of linearized growth rates about several simple geometries. To develop physical understanding, we will begin with an interface in the shape of a straight line; we will then turn to the more experimentally relevant case of a circular boundary.

A. Stability about a line

Consider an unperturbed interface that rests on the line $y=0$ and subject it to a sinusoidal perturbation $\mathbf{r}(x) = \hat{y}(k)e^{ikx}\mathbf{e}_y$, where \mathbf{e}_y is a unit vector in the y -direction; we use the wavevector k to distinguish a one-dimensional Fourier transform from a two-dimensional transform with wavevector q . This gives rise to a force $\Delta \mathbf{f} = \hat{f}(k)e^{ikx}\mathbf{e}_y$ which in turn causes a velocity at the interface $\hat{u}(k)e^{ikx}\mathbf{e}_y$, with $\hat{u} = \partial \hat{y} / \partial t$. For a boundary without internal structure, $\Delta \mathbf{f}$ must always be normally directed, so there is no possibility that it will have an \mathbf{e}_x component. The relationship of \hat{f} to \hat{y} will depend on $\mathcal{E}[\mathbf{r}]$, and its particular form is not of immediate interest in the present discussion. Quite generally, though, we expect that $\hat{u} \propto \hat{f} \propto \hat{y}$. Since \hat{f} is already first order small, once it has been calculated we may consider that the boundary takes its unperturbed shape. In those cases in which an analytic expression for G_{ij} is known, we may then simply calculate the velocity component as

$$\hat{u}(k) = -\frac{\hat{f}(k)}{4\pi\eta} \int_{-\infty}^{\infty} dx G_{22}(x\mathbf{e}_x) e^{ikx}. \quad (28)$$

We find that in the limit of negligible subfluid dissipation ($a \rightarrow 0$),

$$\hat{u}(k) = -\frac{\hat{f}(k)}{4\eta|k|}, \quad (29)$$

while in the case of a thin subfluid,

$$\hat{u}(k) = -\frac{\hat{f}(k)}{2\eta\lambda^2} \left[|k| - \frac{k^2}{\sqrt{k^2 + \lambda^2}} \right], \quad (30)$$

Once again the effects of the subfluid are unimportant at small enough length scales: As $|k|/\lambda \rightarrow \infty$, the expression approaches that valid in the absence of a subfluid. Similarly, as $|k|/\lambda \rightarrow 0$, we recover the form that has previously been calculated starting from Darcy's law.^{22,23}

When a compact direct space form for G_{ij} is not known, one may still find the growth rates by remaining in Fourier space. The method is presented in Appendix C for stability about a circle; the results of a similar calculation for a line are plotted in Figure 2 in terms of a reduced growth rate $\sigma(k) \equiv \hat{u}(k)\eta'/\hat{f}(k)$. At present, we simply state that, for an infinite subfluid in the limit $|k|/a \ll 1$,

$$\hat{u}(k) = -\frac{\hat{f}(k)}{\pi\eta'}. \quad (31)$$

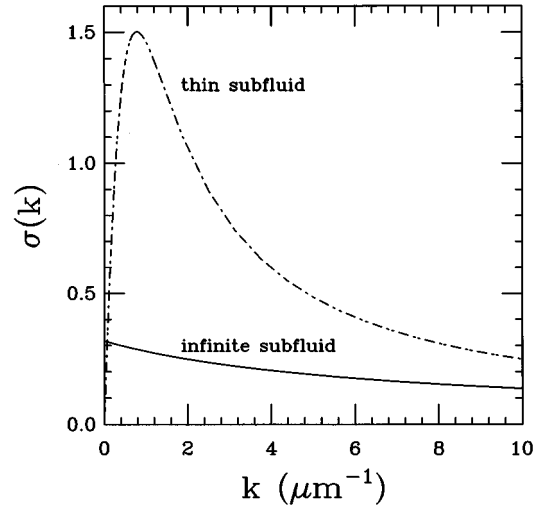


FIG. 2. Comparison of the reduced growth rates $\sigma(k) \equiv \hat{u}(k)\eta'/\hat{f}(k)$ about a line in the limits of a very thin subfluid and of an infinite subfluid. Both curves are for a system with $a = 10\mu\text{m}^{-1}$. The dotted line was calculated using equation (30) with $d = 10\mu\text{m}$; the solid curve was obtained by the methods of Appendix B in the limit $d \rightarrow \infty$. The two curves approach each other and drop off like $1/k$ as $k \rightarrow \infty$, but have markedly different behavior for values of $1/k$ on the order of typical domain length scales.

This is the same k dependence one would expect if dissipation occurred only at the boundary of the domain, instead of in the bulk fluid.

The k dependence of these growth rates can be understood on the basis of relatively simple arguments. Suppose that $\hat{H}(\mathbf{q}) \sim q^n$; n is determined by the number of derivatives of \mathbf{u} and of p in the dynamical equation. Then, we expect that $\hat{G}_{ij} \sim q^{n+2}$. To find the linearized growth rate about a line, one must first take the inverse transform of \hat{G}_{ij} in two dimensions, then, in a rough sense, take a one-dimensional Fourier transform of the resulting function. On purely dimensional grounds, this will introduce an additional factor of q . Identifying q with the wavevector k of the perturbation, we then expect that $\hat{u}(k) \sim k^{n+3}$. This is indeed the case: When $a = 0$, $\hat{H} \sim q^{-4}$ and $\hat{u}(k) \sim k^{-1}$, and similarly for the other limits.

B. Stability about a circle

As in the previous section, we begin by considering a slightly perturbed domain parametrized as $\mathbf{r}(\theta) = R(1 + \epsilon_n e^{in\theta})\mathbf{e}_r$, where \mathbf{e}_r is a radially-directed unit vector. We expect a force $f_n e^{in\theta}\mathbf{e}_r$ and a normal velocity component $u_n e^{in\theta}\mathbf{e}_r$; $u_n = R d\epsilon_n/dt$. The force must again be normally-directed for a structureless interface. Incompressibility requires that the fluid velocity have a tangential component at the interface, unlike in the case of a line; this component does not, however, affect the evolution of the boundary's shape, so we will ignore it. To lowest order, we may still consider that the force acts at the unperturbed circle: Although there can now exist a zeroth order force, it must be independent of θ and so will not cause any fluid motion, even when acting at the perturbed interface.

Whereas for stability about a line we used a variety of direct space forms for G_{ij} , here we shall instead derive one expression valid for arbitrary a and d . We begin by observing that, using polar coordinates and integrating over the polar angle, we may formally write

$$H(\mathbf{r}) = 2\pi \int_0^\infty dq \frac{J_0(qr)}{q^2[q + a \coth(qd)]}. \quad (32)$$

Starting from this representation of H , straightforward but lengthy manipulations (described in Appendix C) lead to an expression for the growth rate u_n :

$$u_n = -\frac{n^2 R f_n}{\eta} \int_0^\infty dw \frac{J_n^2(w)}{w^2[w + aR \coth(wd/R)]}. \quad (33)$$

This is the central result of this section and the analog of the growth rates given by equations (29), (30), and (31) for perturbations about a line. If we let the subfluid be infinite and set $\coth(wd/R) = 1$, we recover the expression previously obtained by Stone and McConnell.¹³ When $a = 0$ or $aR \rightarrow \infty$, the integral can be evaluated in closed form. One finds that

$$u_n = -\frac{R}{4\eta} \frac{|n|}{n^2 - 1} f_n \quad (|n| \geq 2), \quad (34)$$

when dissipation occurs only in the monolayer, and

$$u_n = -\frac{4}{\pi\eta'} \frac{n^2}{4n^2 - 1} f_n \quad (|n| \geq 2), \quad (35)$$

when the subfluid dominates. The leading corrections to these expressions for finite aR can also easily be computed. In both cases, the first correction tends to decrease the magnitude of the growth rate. This is not surprising: To zeroth order, we entirely ignored dissipation in the subfluid, in the one case, and in the monolayer, in the other. The next term, by accounting for these additional sources of energy loss, increases the total amount of damping and so slows down the dynamics.

One may verify that in the limit $n \rightarrow \infty$, $R \rightarrow \infty$, with $k = n/R$ fixed, the results (34) and (35) for a circle tend to the growth rates about a straight line (29) and (31). For n large enough, the curvature of the circular boundary is unimportant on the scales over which the forces and velocities vary, and the boundary acts essentially like a line. Hence, the length scale with which one must compare a is not the circle's radius R but the wavelength of the perturbation, which is proportional to $1/k = R/n$. The expression (34) is the appropriate approximation for small aR/n , while (35) is more accurate for large aR/n . This dependence on n of the dominant source of dissipation can be seen in Fig. 3, where the exact reduced growth rate $\sigma_n \equiv u_n \eta' / f_n$ is compared with the two limiting forms. For fixed $aR \gg 1$, the growth rate is roughly independent of n for small n but decays like $1/n$ for large n . The crossover occurs where the curves given by equations (34) and (35) intersect, at $aR/n \sim 1$. Except for a multiplicative factor, the growth rate about a line is a function only of a/k . This is not precisely the case for a circle, but, even for n small, many important quantities depend essentially only on aR/n . For example, Fig. 4 plots versus aR/n the fractional difference between the exact growth rate

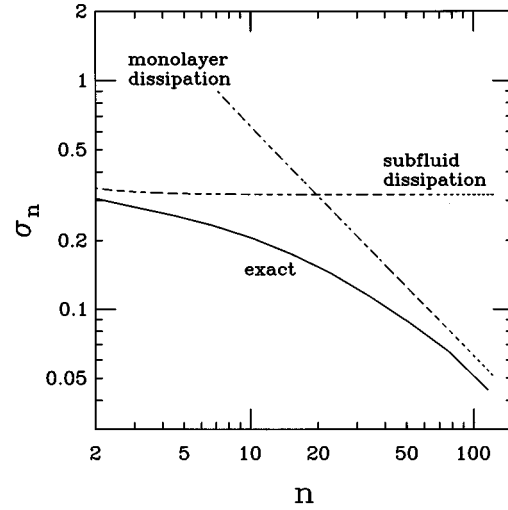


FIG. 3. Reduced growth rate $\sigma_n \equiv u_n \eta' / f_n$ versus the mode number n for a circular domain with $aR = 25$ resting on an infinitely deep subfluid. The solid line gives the exact value, calculated from equation (33). The downward sloping dotted line gives the expression valid when dissipation in the subfluid is negligible [equation (34)], while the other dotted line plots the expression valid in the opposite limit [equation (35)]. The exact growth rate is always less than either of the approximations, but approaches the limiting expressions as $n \rightarrow 2$ and $n \rightarrow \infty$.

given by equation (33) and the approximation of equation (35) for a number of different values of aR and n . To a good approximation, all of the points fall on the same curve. Actually, this collapse occurs over a much wider range of aR/n than shown in the figure, even when the fractional error is greater than $\mathcal{O}(1)$. Figure 4 also gives an idea of the error involved in using the approximate expression for the growth rate. We see that for aR as high as 100, the approxi-

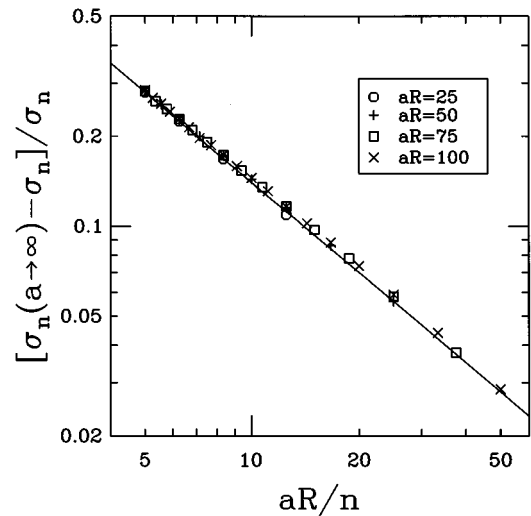


FIG. 4. Fractional error $[\sigma_n(a \rightarrow \infty) - \sigma_n] / \sigma_n$ vs aR/n for a circular domain resting on an infinite subfluid. Here $\sigma_n \equiv u_n \eta' / f_n$ is the reduced growth rate calculated from the exact expression (33), while $\sigma_n(a \rightarrow \infty)$ is obtained from the approximation (35) valid when dissipation in the monolayer can be neglected. The solid line gives the best-fit power law, $[\sigma_n(a \rightarrow \infty) - \sigma_n] / \sigma_n \approx 1.4 / (aR/n)$.

mation is accurate to within 5% for the first few modes, with error increasing linearly as n/aR for larger n . This asymptotic dependence of the error may also be derived directly by expanding the integrand of equation (33).³⁶

C. Example: Dipolar forces

In previous sections, we made no assumptions about the nature of the energy functional $\mathcal{E}[\mathbf{r}]$ associated with the boundary. Here we undertake a sample calculation for the functional of greatest experimental interest, that of a dipolar domain. In this case, we associate with the boundary not only a line tension γ , but also the electrostatic energy stored in the electric field created by the dipoles. In reality, this electric field exerts a force not at the boundary but on the bulk dipolar fluid. Under the assumption that the domain has a constant dipole density, however, the electrostatic body force per unit volume can be written as $-\nabla\phi$, where ϕ is an appropriate potential energy. After the introduction of a modified pressure $p_m = p + \phi$,²⁵ the equations describing the bulk flow are thus unchanged, and the electrostatic interactions only enter through their effect on the boundary conditions. One can show that this effect is correctly incorporated into our formalism if one simply views the electrostatic energy of the dipolar domain as a functional of its boundary's parametrization. Several equivalent forms exist for the energy \mathcal{E}_d of an arbitrarily shaped domain with (constant) dipole density μ per unit area.^{15,21–23,37–40} Of these, the most useful to us takes the form of the energy of interaction of two current loops:

$$\mathcal{E}_d[\mathbf{r}] = -\frac{\mu^2}{h} \int_C ds_1 \int_C ds_2 \hat{\mathbf{t}}(s_1) \cdot \hat{\mathbf{t}}(s_2) \times \Phi\left(\frac{|\mathbf{r}(s_1) - \mathbf{r}(s_2)|}{h}\right). \quad (36)$$

Here C is the curve parametrized by \mathbf{r} , $\hat{\mathbf{t}}$ is the unit tangent to C , h is the thickness of the monolayer, and $\Phi(\xi) = \sinh^{-1}(1/\xi) + \xi - \sqrt{1 + \xi^2}$. Adding to the electrostatic term the usual line tension energy γL , where L is the length of the curve, we arrive at an expression for $\mathcal{E}[\mathbf{r}]$. A fair amount of algebra then yields the force component f_n . In the case of monolayers, the thickness is of molecular size, $h \sim 10\text{\AA}$, and the typical domain radius is $R \sim 10\mu\text{m}$, so we are justified in taking the limit in which the aspect ratio $p \equiv 2R/h \gg 1$. It has then been shown that¹⁵

$$f_n = \frac{\gamma}{R} \left[\left\{ 1 - \frac{1}{2} N_B \ln\left(\frac{8R}{eh}\right) \right\} (n^2 - 1) + \frac{1}{4} N_B (1 - 4n^2) \sum_{j=2}^n \frac{1}{2j-1} \right]. \quad (37)$$

Here the dipolar Bond number $N_B \equiv 2\mu^2/\gamma$ gives the relative importance of the electrostatic and line tension forces. Substituting this expression for f_n into any of the growth rates calculated in the last section, one obtains a prediction for u_n that can be compared directly with experiment. With values of the line tension on the order of 1×10^{-8} erg/cm,¹⁵ a domain radius $R \sim 50\mu\text{m}$, and subfluid viscosity $\eta' = 1$ cp,

we obtain interface velocities on the order of $1 \mu\text{m/s}$ for small N_B , and considerably less near the branching instability.

V. DYNAMICAL LAW FOR MOTION DOMINATED BY THE SUBFLUID

Two important features of the limit in which $aL \rightarrow \infty$ have already been emphasized: First, the monolayer viscosity represents a singular perturbation that must always be taken into account near enough to a boundary or to a singularity. Second, linear stability results suggest that this limit can be partially understood in terms of an effective *local* dissipative force that opposes the boundary velocity at a given point on the interface. It is the purpose of this section to use these two observations to find a simplified boundary integral expression valid as $aL \rightarrow \infty$. The physical ideas that will motivate the discussion are relatively straightforward: The Green's function G_{ij} deviates appreciably from its asymptotic large a form only when $r \lesssim 1/a$. For a large enough, this describes a very small region around the point where we wish to know the boundary velocity, and it seems plausible that one might be able to neglect the variation of physical quantities across this region. Then, the contribution transmitted through the monolayer itself to the velocity at a point \mathbf{r} will be proportional to $\Delta\mathbf{f}(\mathbf{r})$. In this picture, the effective force at the interface is thus a consequence of the extremely small length scales over which dissipation in the monolayer is important. These allow us to take this dissipation to be essentially local compared with the dissipation in the subfluid, which retains its very nonlocal character.

To put these ideas into mathematical form, we begin by finding the limiting forms of G_{ij} for small and large ar . These can be obtained by straightforward differentiation of the corresponding limits of $H(\mathbf{r})$, derived in previous sections and in Appendix II. One finds that for ar small, G_{ij} behaves as

$$G_{ij}^S(\mathbf{r}) = \left[\frac{3}{4} + C + \ln\left(\frac{ar}{2}\right) \right] \delta_{ij} + \frac{r_i r_j}{r^2}, \quad (38)$$

while for ar large the appropriate expression is

$$G_{ij}^L(\mathbf{r}) = \frac{2r_i r_j}{ar^3}. \quad (39)$$

Note the important feature of G_{ij}^L that, unlike most of the Green's functions we have examined, it does not contain a term proportional to δ_{ij} . As a first approximation, we will suppose that there is a sharp transition between small and large ar behavior. That is, we will approximate the full Green's function as

$$G_{ij}(\mathbf{r}) = \begin{cases} G_{ij}^S(\mathbf{r}), & r < v/a, \\ G_{ij}^L(\mathbf{r}), & r > v/a, \end{cases} \quad (40)$$

where v is a constant of order unity that will be determined later. The expression for the velocity at a point \mathbf{r} then becomes

$$u_j(\mathbf{r}) = -\frac{1}{4\pi\eta} \int_{|\mathbf{r}-\mathbf{r}(s)| > v/a} ds G_{ij}^L(\mathbf{r}-\mathbf{r}(s)) \Delta f_i(\mathbf{r}(s)) \\ - \frac{1}{4\pi\eta} \int_{|\mathbf{r}-\mathbf{r}(s)| < v/a} ds G_{ij}^S(\mathbf{r}-\mathbf{r}(s)) \Delta f_i(\mathbf{r}(s)). \quad (41)$$

This expression can be written in an alternative form in the usual case in which there are no tangential forces and one is only interested in the normal velocity. Then, the product $G_{ij}^L \Delta f_i$ is not singular as $\mathbf{r}(s)$ approaches \mathbf{r} because the only nonvanishing term in the sum contains a factor of $[(\mathbf{r}(s)-\mathbf{r}) \cdot \hat{\mathbf{n}}]^2$ in the numerator. Choosing the coordinate $s=0$ when $\mathbf{r}(s)=\mathbf{r}$ and expanding for small s , one finds that $\mathbf{r}(s)-\mathbf{r} \approx \hat{\mathbf{t}}s - (1/2)\kappa \hat{\mathbf{n}}s^2 + \dots$. Hence, $[(\mathbf{r}(s)-\mathbf{r}) \cdot \hat{\mathbf{n}}]^2 \propto s^4$, cancelling the singularity in the denominator of G_{ij}^L and making it possible to extend the integral of G_{ij}^L to zero. For notational convenience, we pick axes such that $\hat{\mathbf{n}}$ and $\hat{\mathbf{t}}$ correspond to \mathbf{e}_x and \mathbf{e}_y , respectively, when $s=0$. Then, the normal component of \mathbf{u} at \mathbf{r} is just u_1 , and we can write

$$u_1(\mathbf{r}) = -\frac{1}{4\pi\eta} \int_{\mathcal{C}} ds G_{i1}^L(\mathbf{r}-\mathbf{r}(s)) \Delta f_i(\mathbf{r}(s)) \\ - \frac{1}{4\pi\eta} \int_{|\mathbf{r}-\mathbf{r}(s)| < v/a} ds [G_{i1}^S(\mathbf{r}-\mathbf{r}(s)) \\ - G_{i1}^L(\mathbf{r}-\mathbf{r}(s))] \Delta f_i(\mathbf{r}(s)). \quad (42)$$

Because G_{ij}^L contains a factor of $1/a$, the first integral in the above expression will be proportional to $1/a$. Thus, to leading order in large a , only terms of order $1/a$ in the second integral are of interest. At this level of approximation, only constant and logarithmic terms in the integrand need be retained—that is, forces and velocities are taken to vary very slowly across the region of integration. Then, the second integral becomes

$$-\frac{1}{4\pi\eta} \int_{-v/a}^{v/a} ds \Delta f_1(\mathbf{r}) \left[\ln\left(\frac{a|s|}{2}\right) + C + \frac{3}{4} \right] \\ = \frac{\Delta f_1(\mathbf{r})v}{2\pi\eta'} \left[\ln\left(\frac{v}{2}\right) + C - \frac{1}{4} \right], \quad (43)$$

where it should be emphasized that $\Delta f_1(\mathbf{r}) = \Delta \mathbf{f}(\mathbf{r}) \cdot \mathbf{e}_x$ is the force component at the point where we wish to calculate the velocity, and so does not depend on s . Hence, to leading order in large a , the second integral yields a local force. We must still, however, specify the numerical value of the proportionality constant $v[\ln(v/2) + C - 1/4]$ in equation (43), or, equivalently, of v itself. This can be done by demanding that the approximations of this section lead to the same linear stability results as the limits as $a \rightarrow \infty$ of the expressions valid for arbitrary a already obtained. Thus we ask that v be such that $\hat{u}(k) = -\hat{f}(k)/\pi\eta'$ [Eq. (31)] for stability about a line, and similarly for other geometries. This requirement determines the unique value $v \approx 2.88$. Likewise, with this choice of v , one can show that the proposed dynamical law preserves the area of domains and that the interfacial velocity of an arbitrarily shaped domain will vanish when the force is

constant and normally-directed, both very desirable features. Substituting for v , we find the approximation to equation (7) that is the central result of this section:

$$u_1(\mathbf{r}) = -\frac{\Delta f_1(\mathbf{r})}{\pi\eta'} - \frac{1}{4\pi\eta} \int_{\mathcal{C}} ds G_{i1}^L(\mathbf{r}-\mathbf{r}(s)) \Delta f_i(\mathbf{r}(s)). \quad (44)$$

The first term can be associated with dissipation in the monolayer and is entirely local, while the second corresponds to dissipation in the subfluid. Note that the factor of $1/a$ in G_{ij}^L , when multiplied by the $1/\eta$ in front of the integral, yields $1/\eta'$, so the velocity does not depend at all on the monolayer viscosity.

It remains to clarify when the results of this section are expected to hold—that is, what it means for a to be large. By considering the corrections of order $1/a^2$ to the expression (43), one can convince oneself that these are negligible only when

$$a \gg \kappa \quad \text{and} \quad a \gg \frac{\Delta f'_1(\mathbf{r})}{\Delta f_1(\mathbf{r})}, \quad (45)$$

where κ is the curvature, $\Delta f'_1 \equiv d(\Delta \mathbf{f}(\mathbf{r}(s)) \cdot \mathbf{e}_x)/ds$, and both quantities are evaluated at \mathbf{r} . These expressions are not surprising: For smooth interfaces, the curvature will be of the order of $1/L$, where L is the size of the domain; $\Delta f'_1/\Delta f_1$ gives the length scale over which the force varies. As we have already pointed out, both are important length scales in the system.

Unlike the Green's function valid for arbitrary a , G_{ij}^L has a compact analytic expression in direct space. The formula (44) thus presents considerable advantages for analytic and especially for numerical calculations. Such a simplification is all the more welcome because almost all experiments to date have been performed on systems where the subfluid viscosity dominates. Admittedly, these improvements come at the expense of an approximation that is not perfectly controlled, but that nonetheless appears physically reasonable.

VI. EVOLUTION OF THE PERIMETER

Finally, we provide a simple illustration of the use of the present formulation for calculations in the nonlinear regime. We consider a domain with only line tension energy, $\mathcal{E} = \gamma L$, and calculate the time derivative of its perimeter L . This quantity is of particular interest because L can be observed directly in experiments.

Parametrizing the curve \mathcal{C} in the standard way as $\mathbf{r}(\alpha)$, and recalling that $\delta L/\delta \mathbf{r}(\alpha) = -d\hat{\mathbf{t}}/d\alpha$, we can write

$$\frac{dL}{dt} = -\gamma \int_{\mathcal{C}} d\alpha \frac{d\hat{\mathbf{t}}}{d\alpha} \cdot \mathbf{u}(\alpha) = -\frac{\gamma}{4\pi\eta} \int_{\mathcal{C}} ds_1 \int_{\mathcal{C}} ds_2 \kappa(s_1) \\ \times n_i(s_1) G_{ij}(\mathbf{r}_{12}) \kappa(s_2) n_j(s_2), \quad (46)$$

where $\mathbf{r}_{12} = \mathbf{r}(s_1) - \mathbf{r}(s_2)$, κ is the curvature, and s is the arclength parameter. Since $\mathcal{E} \propto L$, it will always be true that $dL/dt < 0$; the proof is identical to that already given for an arbitrary energy functional. The Green's function G_{ij} can be

any of the several forms we have already presented. One could equally use the approximate form (44) of the previous section for the velocities, finding that

$$\frac{dL}{dt} = -\frac{\gamma}{\pi\eta'} \int_{\mathcal{C}} ds \kappa^2 - \frac{\gamma}{4\pi\eta} \int_{\mathcal{C}} ds_1 \int_{\mathcal{C}} ds_2 \kappa(s_1) \times n_i(s_1) G_{ij}^L(\mathbf{r}_{12}) \kappa(s_2) n_j(s_2), \quad (47)$$

when the monolayer viscosity is small. These expressions for dL/dt are the analogs of the area-conserving “curve-shortening equation” previously derived, under the assumption that dissipation occurs only at the domain boundary.²¹ This simpler equation has already been fruitfully compared with experiment,^{9,15} and we hope that our extensions will likewise prove useful in analyzing data.

VII. DISCUSSION

Equation (7) encapsulates the focus of this paper: It provides a general prescription for finding the velocity of the boundary of an arbitrarily shaped monolayer domain. We have discussed the form this equation takes in several limiting cases and have shown that it can be used to make quantitative predictions that can be compared with experiment. In particular, section V suggests an approach to the limit in which dissipation in the monolayer itself is small; since most experiments have been conducted in this regime,^{12,30} its dynamics are of particular interest. Our approximation to equation (7) has the interesting feature that it contains a local term whose effect is equivalent to that of a drag force acting directly on the interface. From a theoretical perspective, it is clear that our somewhat *ad hoc* treatment of this limit leaves a number of open questions. For example, the issue of whether the dynamical law (44) gives precisely a gradient flow demands further elucidation, as does the application of our arguments to the case of a thin subfluid, which seems to reduce to Darcy’s law when the subfluid viscosity dominates. In general, a more mathematically rigorous treatment is desirable. These problems are currently under active study.⁴¹ The logical next step would be to undertake a detailed numerical investigation of relaxation and pattern formation in the strongly nonlinear regime; techniques that have been developed for similar problems²⁵ should make such studies possible. To provide a complete test of the theory, it likewise seems useful to conduct experiments on systems in which the monolayer viscosity is sufficiently large that it can be measured independently.^{42,43} Experiments carried out on a shallow trough might also be of interest. Finally, there are several physical effects that our theory does not pretend to include. Foremost among these are, first, the possibility that one of the monolayer phases might have a significant compressibility, and, second, the presence of thermal fluctuations in domain shape. The inclusion of thermal fluctuations, in particular, might have a significant qualitative effect on the pattern-forming properties of the model. We also have made no attempt to treat the dynamics of the various liquid condensed phases that show hexatic or other long-range order. Clearly, such order greatly increases the complexity of the problem.

ACKNOWLEDGMENTS

We thank M. Gannon, E. K. Mann, and M. J. Shelley for helpful discussions. We are especially grateful to H. A. Stone for a careful reading of a late version of the manuscript and for making available the numerical routines used in generating Fig. 4. This work was supported in part by a Barry M. Goldwater Scholarship and a NSF Graduate Research Fellowship (DKL), and by a NSF Presidential Faculty Fellowship DMR93-50227 and the Alfred P. Sloan Foundation (REG).

APPENDIX A: DETAILS OF THE DERIVATION OF THE GREEN’S FUNCTION

This appendix gives a few of the steps that were omitted in the main text in the derivations of equations (11) and (12). Since the components of \mathbf{u}' are harmonic, they can be represented in the usual manner as

$$u'_i(\mathbf{r}_0) = -\frac{1}{4\pi} \int d^2\mathbf{r} u_i(\mathbf{r}) \frac{\partial \mathcal{G}(\mathbf{r}, \mathbf{r}_0)}{\partial z}, \quad (A1)$$

where \mathcal{G} is a Green’s function for Laplace’s equation that vanishes on the plane $z=0$, and the integral is taken over this plane.²⁹ The boundary conditions are that $\mathbf{u}'_{\perp} = \mathbf{u}$ at $z=0$, so the two-dimensional velocity components u_i appear in the integrand. The Green’s function \mathcal{G} is obtained by an eigenfunction expansion in Cartesian coordinates. With the hat denoting a Fourier transform with respect to the variables $x-x_0$ and $y-y_0$, one finds that

$$\hat{\mathcal{G}}(\mathbf{q}, z, z_0) = -\frac{1}{\pi q} \frac{\sinh(qz_{>}) \sinh[q(z_{<} + d)]}{\sinh(qd)}, \quad (A2)$$

where $z_{>}$ and $z_{<}$ are, respectively, the larger and smaller of z and z_0 . Since $\mathbf{F}^S = -\eta' \partial \mathbf{u}'_{\perp} / \partial z$, comparison of equations (11) and (A1) indicates that $\hat{K} = \partial^2 \hat{\mathcal{G}} / \partial z \partial z_0$, with the derivatives evaluated at $z=z_0=0$. The expression (12) for \hat{K} follows immediately.

APPENDIX B: INVERSION OF \hat{H}

In this appendix, we obtain an analytic expression for the inverse transform of $\hat{H} = 1/[q^3(q+a)]$. Begin by expanding in partial fractions:

$$\hat{H}(\mathbf{q}) = \frac{1}{aq^3} - \frac{1}{a^2q^2} + \frac{1}{a^3q} - \frac{1}{a^3(q+a)}. \quad (B1)$$

The inverse transforms of the first three terms are known.³³ To invert the fourth, we use the general result that $\mathcal{F}^{-1}[g(\mathbf{q})] = -(1/r^2) \mathcal{F}^{-1}[\nabla_q^2 g(\mathbf{q})]$, where \mathcal{F}^{-1} denotes an inverse Fourier transform and the derivatives in the Laplacian are taken with respect to q . We can then write

$$H(\mathbf{r}) = \frac{2\pi}{a^2} \left[-\xi + \ln \xi + \frac{1}{\xi} + \frac{1}{\xi^2} \int_0^\infty dx J_0(\xi x) \frac{x-1}{(x+1)^3} \right]. \quad (B2)$$

Here, we have expressed the result in a dimensionless form by setting $\xi = ar$ and have performed the integral over the polar angle in the inverse transform of $\nabla_q^2 [1/(q+a)]$. The integral in the fourth term converges in the usual sense and

so can be evaluated numerically. It can also be expressed analytically in terms of a rather lengthy expression involving generalized hypergeometric functions ${}_pF_s$. These have known Taylor expansions that converge everywhere in the complex plane.⁴⁴ The expansions lead directly to the series (22). It can also be shown that to leading order for large ξ , $H(\mathbf{r}) = -2\pi\xi/a^2$, as one would expect from the limiting form of the Fourier transform for small q .

APPENDIX C: LINEAR STABILITY CALCULATION FOR A CIRCLE

We take as our starting point the integral expression (32) for $H(\mathbf{r})$. Differentiating under the integral sign, we find that

$$\begin{aligned} G_{ij}(\mathbf{r}) &= 2\pi \int_0^\infty dq \frac{D_{ij}J_0(qr)}{q^2[q + a \coth(qd)]} \\ &= -2 \int_0^\infty \frac{dq}{q^2[q + a \coth(qd)]} \\ &\quad \times \left[\left(\delta_{ij} - \frac{r_i r_j}{r^2} \right) q^2 J_0''(qr) + \frac{r_i r_j}{r^3} q J_0'(qr) \right]. \quad (C1) \end{aligned}$$

In order to find u_n , we calculate the velocity at $\theta=0$. Parametrizing the curve as $\mathbf{r}(\theta) = R(\cos\theta \mathbf{e}_x + \sin\theta \mathbf{e}_y)$, we may write the velocity in the usual manner as the integral around the curve of the Green's function multiplied by the force

$$\begin{aligned} u_n &= -\frac{Rf_n}{4\pi\eta} \int_0^{2\pi} d\theta G_{1j}(R[(1-\cos\theta)\mathbf{e}_x \\ &\quad - \sin\theta\mathbf{e}_y]) e^{in\theta} \mathbf{e}_{r,j}, \quad (C2) \end{aligned}$$

where $\mathbf{e}_{r,j}$ is a component of \mathbf{e}_r . Substituting the integral expression (C1) for G_{ij} , setting $w \equiv qR$, and performing some algebraic manipulations, one finds that

$$\begin{aligned} u_n &= \frac{f_n}{\pi\eta R} \int_0^\infty \frac{dq}{q^2[q + a \coth(qd)]} \int_0^\pi d\phi \cos(2n\phi) \\ &\quad \times \left[\frac{wJ_1(2w\sin\phi)}{2\sin\phi} - w^2 \cos^2\phi J_0(2w\sin\phi) \right]. \quad (C3) \end{aligned}$$

The identity $\pi J_n(z)^2 = \int_0^\pi d\phi J_0(2z\sin\phi)\cos(2n\phi)$ ⁴⁴ and two integrations by parts enable one to evaluate the integral with respect to ϕ . The growth rate given in Sec. IV is then obtained by changing variables of integration from q to w . The same approach can also be applied to other geometries.

¹H. Möhwald, "Phospholipid and phospholipid-protein monolayers at the air-water interface," *Annu. Rev. Phys. Chem.* **41**, 441 (1990).

²H. M. McConnell, "Structures and transitions in lipid monolayers at the air-water interface," *Annu. Rev. Phys. Chem.* **42**, 171 (1991).

³M. Seul and D. Andelman, "Domain shapes and patterns: The phenomenology of modulated phases," *Science* **267**, 476 (1995).

⁴M. Seul and M. J. Sammon, "Competing interactions and domain-shape instabilities in a monomolecular film at an air-water interface," *Phys. Rev. Lett.* **64**, 1903 (1990).

⁵M. Seul, "Domain wall fluctuations and instabilities in monomolecular films," *Physica A* **168**, 198 (1990).

⁶K. J. Stine, C. M. Knobler, and R. C. Desai, "Buckling instability in monolayer network structures," *Phys. Rev. Lett.* **65**, 1004 (1990).

⁷D. J. Benvegnu and H. M. McConnell, "Line tension between liquid domains in lipid monolayers," *J. Phys. Chem.* **96**, 6820 (1992).

⁸E. K. Mann, S. Hénon, D. Langevin, and J. Meunier, "Molecular layers of

a polymer at the free water surface: Microscopy at the Brewster angle," *J. Phys. II* **2**, 1683 (1992).

⁹M. Seul, "Dynamics of domain shape relaxation in Langmuir films," *J. Phys. Chem.* **97**, 2941 (1992).

¹⁰K. J. Stine and D. T. Stratmann, "Fluorescence microscopy study of Langmuir monolayers of stearylamine," *Langmuir* **8**, 2509 (1992).

¹¹K. Y. C. Lee and H. M. McConnell, "Quantized symmetry of lipid monolayer domains," *J. Phys. Chem.* **97**, 9532 (1993).

¹²E. K. Mann, S. Hénon, D. Langevin, J. Meunier, and L. Léger, "The hydrodynamics of domain relaxation in a polymer layer," *Phys. Rev. E* **51**, 5708 (1995).

¹³H. A. Stone and H. M. McConnell, "Hydrodynamics of quantized shape transitions in lipid domains," *Proc. R. Soc. London Ser. A* **448**, 97 (1995).

¹⁴H. A. Stone and H. M. McConnell, "Lipid domain instabilities in monolayers overlying sublayers of finite depth," *J. Phys. Chem.* **99**, 13505 (1995).

¹⁵R. E. Goldstein and D. P. Jackson, "Domain shape relaxation and the spectrum of thermal fluctuations in Langmuir monolayers," *J. Phys. Chem.* **98**, 9626 (1994).

¹⁶B. D. Hughes, B. A. Pailthorpe, and L. R. White, "The translational and rotational drag on a cylinder moving in a membrane," *J. Fluid Mech.* **110**, 349 (1981).

¹⁷D. K. Schwartz, C. M. Knobler, and R. Bruinsma, "Direct observation of Langmuir monolayer flow through a channel," *Phys. Rev. Lett.* **73**, 2841 (1994).

¹⁸H. A. Stone, "Fluid motion of monomolecular films in a channel flow geometry," *Phys. Fluids* (in press).

¹⁹A. O. Tsebers and M. M. Maiorov, "Magnetostatic instabilities in plane layers of magnetizable liquids," *Magnetohydrodynamics* **16**, 21 (1980).

²⁰A. O. Tsebers and A. A. Zemitis, "Numerical simulation of MHD instability in the free surface of a gripped drop of magnetic liquid. Part 1," *Magnetohydrodynamics* **19**, 360 (1983).

²¹S. A. Langer, R. E. Goldstein, and D. P. Jackson, "Dynamics of labyrinthine pattern formation in magnetic fluids," *Phys. Rev. A* **46**, 4894 (1992).

²²A. J. Dickstein, S. Erramilli, R. E. Goldstein, D. P. Jackson, and S. A. Langer, "Labyrinthine pattern formation in magnetic fluids," *Science* **261**, 1012 (1993).

²³D. P. Jackson, R. E. Goldstein, and A. O. Cebers, "Hydrodynamics of fingering instabilities in dipolar fluids," *Phys. Rev. E* **50**, 298 (1994).

²⁴T. Chou and D. R. Nelson, "Surface wave scattering at nonuniform fluid interfaces," *J. Chem. Phys.* **101**, 9022 (1994); T. Chou, S. K. Lucas, and H. A. Stone, "Capillary wave scattering from a surfactant domain," *Phys. Fluids A* **7**, 1872 (1995).

²⁵C. Pozrikidis, *Boundary Integral and Singularity Methods for Linearized Viscous Flow* (Cambridge University Press, Cambridge, 1992).

²⁶M. Doi and S. F. Edwards, *The Theory of Polymer Dynamics* (Oxford University Press, Oxford, 1986).

²⁷It is well-known that high Reynolds number flows can be treated as incompressible when typical flow velocities are much less than the speed of sound in the fluid. One can readily show that the analogous criterion for low Reynolds number flow in which dissipation in the subfluid dominates is $\eta'U\beta \ll 1$, where U is a typical velocity and β is the compressibility of the monolayer. Denser liquid-like phases easily satisfy this condition, in agreement with the observation that domain areas generally remain constant to within experimental error.^{9,12} It is not usually possible, however, to measure the compressibility of the considerably less dense gas-like phases that are present in some experimental systems, so one can legitimately question whether it is valid to treat them as incompressible.

²⁸P. G. Saffman, "Brownian motion in thin sheets of viscous fluid," *J. Fluid Mech.* **73**, 593 (1976).

²⁹J. D. Jackson, *Classical Electrodynamics*, 2nd ed. (Wiley, New York, 1975), pp. 43–44.

³⁰J. F. Klinger and H. M. McConnell, "Brownian motion and fluid mechanics of lipid monolayer domains," *J. Phys. Chem.* **97**, 6096 (1993).

³¹J. F. Klinger and H. M. McConnell, "Field-gradient electrophoresis of lipid domains," *J. Phys. Chem.* **97**, 2962 (1993).

³²M. J. Lighthill, *Introduction to Fourier Analysis and Generalised Functions* (Cambridge University Press, Cambridge, 1958).

³³D. S. Jones, *The Theory of Generalised Functions*, 2nd ed (Cambridge University Press, Cambridge, 1982).

³⁴H. Hasimoto and O. Sano, "Stokeslets and eddies in creeping flow," *Annu. Rev. Fluid Mech.* **12**, 335 (1980).

³⁵I. D. Howells, "Drag due to the motion of a Newtonian fluid through a

- sparse random array of small fixed objects," J. Fluid Mech. **64**, 449 (1974).
- ³⁶H. A. Stone (personal communication).
- ³⁷D. J. Keller, J. P. Korb, and H. M. McConnell, "Theory of shape transitions in two-dimensional phospholipid domains," J. Phys. Chem. **91**, 6417 (1987).
- ³⁸A. O. Cebers, "Labyrinthine structures of magnetic fluids and their electrostatic analogs," Magnetohydrodynamics **25**, 149 (1989).
- ³⁹H. M. McConnell, "Harmonic shape transitions in lipid monolayer domains," J. Phys. Chem. **94**, 4728 (1990).
- ⁴⁰J. M. Deutch and F. E. Low, "Theory of shape transitions of two-dimensional domains," J. Phys. Chem. **96**, 7097 (1992).
- ⁴¹D. K. Lubensky (unpublished).
- ⁴²N. L. Jarvis, "Surface viscosity of polydimethylsiloxane monolayers," J. Phys. Chem. **70**, 3027 (1966).
- ⁴³M. Sacchetti, H. Yu, and G. Zograf, "Hydrodynamic coupling of monolayers with subphase," J. Chem. Phys. **99**, 563 (1993).
- ⁴⁴I. S. Gradshteyn and I. M. Ryzhik, *Tables of Integrals, Series, and Products* (Academic Press, San Diego, 1965).